

哀牢山深变质带内两类晚渐新世花岗岩 成因及其构造指示*

郭小飞^{1,2,3}, 王岳军^{2,4}, 刘汇川^{2,4}, 张玉芝^{2,4}

- (1. 中国科学院广州地球化学研究所同位素地球化学国家重点实验室, 广东 广州 510640;
2. 中山大学地球科学与工程学院, 广东 广州 510275;
3. 中国科学院大学, 北京 100049;
4. 广东省地球动力作用与地质灾害重点实验室, 广东 广州 510275)

摘要: 红河-哀牢山构造带发育了广泛的、与印度欧亚板块碰撞造山作用紧密相关的新生代构造-岩浆作用, 出露于云南哀牢山变质带中段的两个花岗岩样品锆石 U-Pb 定年结果分别为 26.2 ± 0.5 Ma 和 26.8 ± 0.5 Ma, 说明哀牢山变质带并不全是扬子板块结晶基底的元古界, 也存在新生代岩浆岩。花岗岩锆石 $\varepsilon_{\text{Hf}}(t)$ 分别为 $+0.3 \sim +6.9$ 和 $-9.8 \sim -0.7$, 平均为 $+3.4$ 和 -4.3 , 其二阶段模式年龄 T_{DM2} 分别为 $526 \sim 853$ Ma 和 $903 \sim 1355$ Ma。低 $\varepsilon_{\text{Hf}}(t)$ 花岗岩源岩可能是元古宙哀牢山群变质杂砂岩, 高 $\varepsilon_{\text{Hf}}(t)$ 花岗岩源自软流圈地幔热源加热诱发的新生下地壳部分熔融。结合前人研究成果, 认为晚渐新世红河剪切带剪切作用切穿了岩石圈地幔; 渐新世印支地块两侧的高黎贡山和哀牢山走滑剪切系统肢解了东南亚不同的块体, 为印支地块向东南方向的挤出创造了条件。

关键词: 哀牢山构造带; 花岗质岩石; 锆石年龄; Hf 同位素; 走滑剪切; 挤出效应

中图分类号: P588.121 文献标志码: A 文章编号: 0529-6579(2017)06-0001-14

Petrogenesis of two types of late Oligocene granites in Ailaoshan tectonic zone and their tectonic implications

GUO Xiaofei^{1,2,3}, WANG Yuejun^{2,4}, LIU Huichuan^{2,4}, ZHANG Yuzhi^{2,4}

- (1. State Key Laboratory of Isotope Geochemistry, Guangzhou Institute of Geochemistry, Chinese Academy of Sciences, Guangzhou 510640, China;
2. School of Earth Sciences and Engineering, Guangzhou 510275, China;
3. University of Chinese Academy of Sciences, Beijing 100049, China;
4. Guangdong Provincial Key Lab of Geodynamics and Geohazards, Sun Yat-sen University, Guangzhou 510275, China)

Abstract: The widespread Cenozoic magmatism in the Red River-Ailaoshan tectonic zone is closely related to the Indian-Eurasian plate collision orogeny. Zircon U-Pb dating results of two granitic samples exposed in the middle part of the Ailaoshan metamorphic belt are 26.2 ± 0.5 Ma and 26.8 ± 0.5 Ma, respectively. This indicates that the Ailaoshan metamorphic zone is not entirely attributed to the Proterozoic crystalline basement of the Yangtze block, while it also contains Cenozoic magmatic rocks. Zircon $\varepsilon_{\text{Hf}}(t)$

* 收稿日期: 2016-10-20

基金项目: 国家重点研发计划项目(2016YFC0600303); 国家重点基础研究发展计划(973)项目(2014CB440901); 国家自然科学基金联合基金(U170160005); 中山大学高校基本业务费项目

作者简介: 郭小飞(1990年生),男;研究方向:构造地质学;E-mail: niubidbrsr@126.com

通信作者: 刘汇川(1986年生),男;研究方向:构造地质学;E-mail: liuhuichuan1986@126.com

values of the samples range from +0.3 to +6.9 and from -9.8 to -0.7 with mean values of +3.4 and -4.3, respectively and their corresponding two-stage Hf model ages (T_{DM2}) range from 526 to 853 Ma and from 903 to 1 355 Ma. The high $\varepsilon_{Hf}(t)$ granites were derived from partial melting of juvenile crust induced by the asthenospheric mantle heat source, while low $\varepsilon_{Hf}(t)$ granites from Proterozoic metamorphic sandstones of the Ailaoshan group. In combination with previous research results, we suggest that the Red River fault has cut across the lithosphere mantle. In SE Asia, the Gaoligongshan and Ailaoshan strike-slip shear zones on both sides of Indosinian block dismembered different blocks and created conditions for their Oligocene extrusion to the southeast.

Key words: Ailaoshan tectonic zone; granitic rocks; zircon ages; Hf isotope; strike slip shear; extrusion effect

我国滇西三江造山带属于东特提斯洋构造域的重要组成部分,经历了复杂的原、古、新三期特提斯洋演化过程^[1-6],是由一系列从冈瓦纳大陆北缘分离出来的外来陆块组成的多岛洋俯冲-碰撞造山带^[7-11]。该构造带在喜山期印度板块与欧亚板块俯冲碰撞作用下于始新世-中新世发育了多条大规模走滑剪切带^[12-14],并随着新生代以来陆内造山带的构造应力调整,形成了滇西地区复杂的地质构造现象。

哀牢山构造带位于三江造山带东南部,带内广泛发育了新元古代-晚古生代-中生代和新生代构造-岩浆作用^[15-20]。红河剪切带新生代剪切作用强烈改造了哀牢山地区的构造-岩浆特征,形成了哀牢山深变质岩带(即哀牢山群)。哀牢山群一直被认为形成于元古代,是扬子地台结晶基底的一部分,但是 Liu et al.^[19]在哀牢山群内识别出了晚三叠世花岗岩,进而提出哀牢山群可能是包含多期次岩浆岩和变质岩的混杂岩带,那么哀牢山群是否也包含新生代红河剪切作用诱发的岩浆岩呢?此外,当前关于红河剪切带研究另一个重要争论在于该剪切作用是否切穿了岩石圈地幔,因为该问题不仅关乎沿剪切带发育的三江地区富碱斑岩 Cu-Mo-Au 多金属矿产的成因,还对印支地块东南向的挤出作用和南海的打开具有重要的指示意义。前人对哀牢山红河剪切带开展了运动学和构造变形的分析,也对剪切带伴生的变质岩开展了变质、变形时代的研究^[21-23]。但是对其中新生代岩浆岩研究尚存争论,而新生代岩浆岩,尤其是记录下地壳甚至深部地幔活动的岩浆岩报道较少,本文对云南省红河州甲寅地区出露的两类花岗质岩石开展了 LA-ICP-MS 锆石 U-Pb 年代学和 Lu-Hf 同位素的分析,以期对红河左旋走滑剪切作用在渐新世是否切穿岩石圈地幔,以及印支地块向东南方向的挤出过程提供资料。

1 地质背景和样品特征

哀牢山-红河变质带夹持于东西两侧的红河断裂和哀牢山断裂之间,是分隔印支地块和扬子地块的一条重要地质界线(图 1)^[26-27]。变质带主体呈北西-南东向延伸,宽度在 20~30 km,长度超过 500 km。变质带内遭受变质变形作用的深变质岩系从北西到南东依次包括点苍山群、哀牢山群、瑶山群和越北的大象山群,主要由斜长角闪岩、片麻岩、大理岩等及后期侵位的岩浆岩组成^[7]。前人研究中普遍把哀牢山群归属于下元古界,认为其属于扬子基底的一部分或者与扬子基底具有相似性^[17,28-30],然而随着锆石 U-Pb 定年等高精度同位素年代学技术的发展和运用,许多原来认为是元古代的花岗岩侵入体,如今被证明属中生代或新生代的变质-变形花岗岩^[16,19,31-33]。研究区哀牢山变质带主体由哀牢山群和部分瑶山群变质岩系组成,为一套混合岩化强烈的中深变质岩,沿哀牢山脉呈 NW-SE 向狭窄带状展布,两侧分别被哀牢山断裂和红河断裂所限,北延至南涧县密滴附近,被红河断裂所切,使哀牢山断裂尖灭,南延入越南范士版带^[34-35]。变质带主体由东西两个变质带构成,即东部的高级变质岩和西部的低级变质岩。高级变质岩带由角闪岩-绿片岩相的片麻岩、角闪岩、大理岩和花岗岩组成,带内因受剪切带活动影响岩石已强烈糜棱岩化。低级变质带由低绿片岩相片岩、千枚岩和板岩等浅变质作用的早古生代碎屑岩组成。两者被一逆冲断裂分隔开,断裂大体沿山脉的主脊延伸^[36]。大部分片麻岩与斜长角闪岩片理化良好且平行于剪切带方向,运动学标志指示左旋剪切。由于变质变形作用的叠加改造,加之混合岩化强烈,原岩面貌和层理特征基本消失,岩性复杂。

本文所研究的 2 个花岗质岩石样品(10HH-

99B、10HH-105B) 位于哀牢山红河剪切带中段滇西红河甲寅地区。10HH-99B 采样坐标 (N 23° 14' 18.9", E 102° 24' 33.2"), 岩石类型为糜棱状变形花岗岩, 样品呈灰色, 糜棱状结构, 块状构造。岩石内部的长英质矿物被压扁拉长形成线理, 面理产状与区域性走滑面理产状一致 (图 2a)。由斜长石、钾长石、石英和少量黑云母、磁铁矿、榍石和锆石等矿物组成。石英因动态重结晶而发生晶体颗粒细粒化, 斜长石表现出明显的环带结构, 黑云母呈细小的鳞片状分布在长石和石英的颗粒边界

(图 2b)。10HH-105B 采样坐标 (N 23° 18' 34.6", E 102° 24' 58.2"), 岩石类型为混合岩化浅色花岗岩脉, 其基质为花岗片麻岩。样品所在的长英质脉体与岩石片麻理平行, 脉体未发生明显变形, 产出方向与剪切带构造面理方向一致。在野外可见长英质脉体被发育于更晚阶段的花岗质脉体侵入, 二者呈现显著截切关系 (图 2c)。浅色花岗岩脉呈白色, 块状构造, 主要矿物为斜长石、钾长石、石英和少量黑云母、磁铁矿、榍石和锆石等 (图 2d), 可见长英质矿物的波状消光。

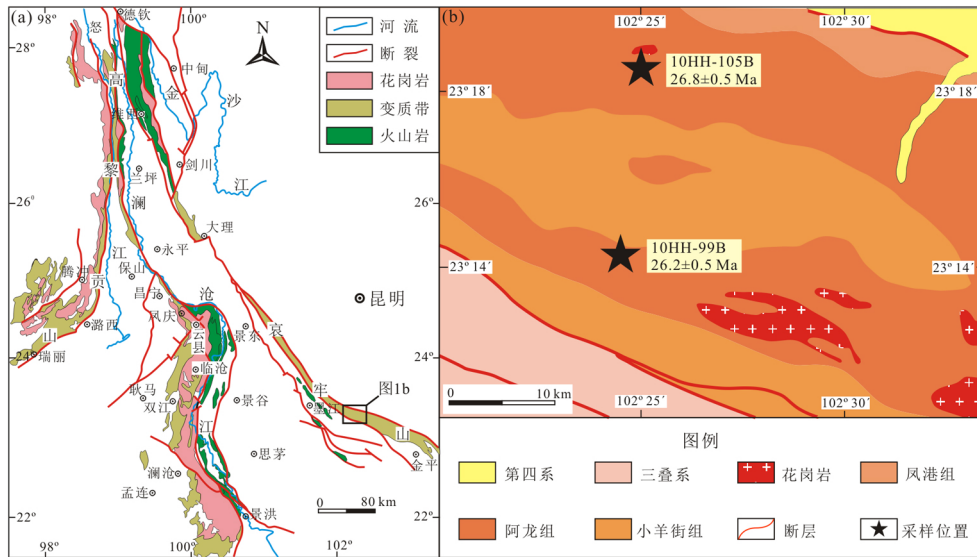


图 1 (a) 哀牢山红河剪切带构造纲要图 (据 [24-25] 修改); (b) 甲寅地区地质简图
 Fig. 1 (a) Tectonic outline map of Ailaoshan-Red River shear zone and (b) geological map of the Jiayin area

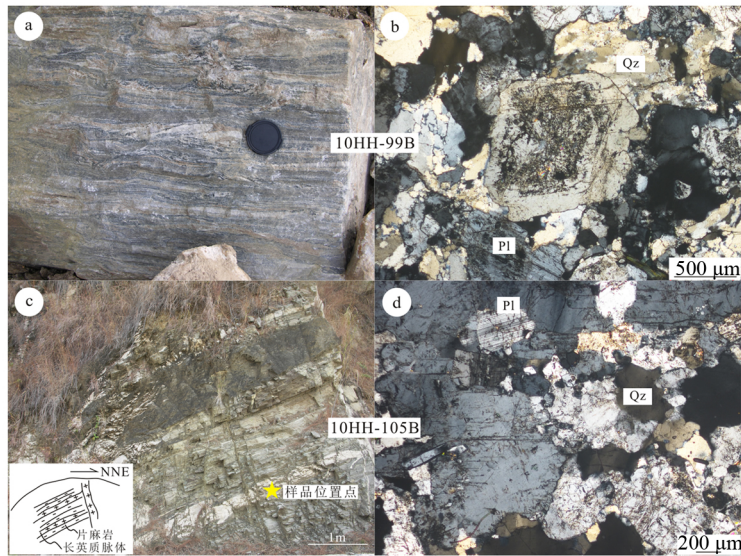


图 2 哀牢山红河剪切带花岗质岩石 10HH-99B 和 10HH-105B 野外照片 (a 和 c) 及正交偏光 (10×4) 显微照片 (b 和 d, Qz - 石英, Pl - 斜长石)
 Fig. 2 Field photos (a and c) and microphotographs (b and d) for granitic rocks of 10HH-99B and 10HH-105B from Ailaoshan-Red River shear zone

2 分析方法

锆石通过重选和磁选技术从新鲜的样品中分选出来,用双目显微镜挑选出无裂隙、无包体、透明干净的锆石颗粒,在玻璃板上用环氧树脂固定、抛光,然后进行反射光和透射光照相,并进行阴极发光 (CL) 图像分析以检查锆石内部结构。锆石 U-Pb 年龄及 Lu-Hf 同位素分析在中国科学院地质与地球物理研究所岩石圈演化国家重点实验室的 Neptune 型多接收电感耦合等离子体质谱仪 (MC-ICP-MS)、Agilent7500a 型四级杆电感耦合等离子体质谱仪 (Q-ICPMS) 和 193 nm 的 ArF 准分子激光系统上进行原位测定完成。详细的分析流程和原理参见^[37-39]。数据处理采用 Ludwig 2001 SQUID 1.02 及 ISOPLOT 程序^[40]。锆石 U-Pb 同位素比值计算采用标准样品 91500 作外标进行校正,分馏校正及计算结果采用 ICPMSDataCal (8.4)^[41]。

3 分析结果

3.1 锆石 U-Pb 年代学

从云南红河甲寅地区 2 个花岗岩样品中挑选出的锆石 CL 图像如图 3 所示,2 个样品的 LA-ICP-MS 锆石 U-Pb 分析结果见表 1 和图 4。

10HH-99B 样品锆石呈自形或半自形长柱状,长度 50 ~ 120 μm 。依据锆石 CL 图像可分出明暗两种锆石,大部分为具有明显岩浆震荡环带的暗色锆石,亮色锆石则呈弱分带或者无分带特点 (图 3a)。此外,部分锆石具有亮色核和暗色边的核边结构,为具有老核新壳的岩浆复合型锆石。此类锆石的新壳具有岩浆锆石所具有的特点,其新壳年龄反映了岩体的结晶时间,老核的年龄为深部地质体提供的信息^[16,42]。对糜棱状变形花岗岩 (10HH-99B) 中的 18 个锆石颗粒进行了分析,所选测点晶形较好,无裂纹和包裹体。其中 12 个测点为暗色锆石颗粒,具有较高的 U 含量。这些锆石的 Th/U 比值在 0.11 ~ 0.20 变化,它们的²⁰⁶Pb/²³⁸U 加权平均年龄值为 $26.2 \pm 0.5 \text{ Ma}$ (MSWD = 0.94; 图 4a)。另外有 2 个测点 18 和 21 为亮色锆石, Th/U 比值分别为 0.60 和 0.19,对应表面年龄为 $40.1 \pm 2.8 \text{ Ma}$ 和 $40.0 \pm 2.1 \text{ Ma}$,可能反映了 ~ 40 Ma 的变质事件; 剩余的 5 个测点也为亮色锆石, Th/U 比值变化于 0.20 ~ 1.54,表面年龄在 190 ~ 699 Ma 之间,代表继承锆石年龄。我们认为,12 个测点的加权平均年龄值 $26.2 \pm 0.5 \text{ Ma}$ 代表糜棱状变形花岗岩的岩浆结晶年龄。

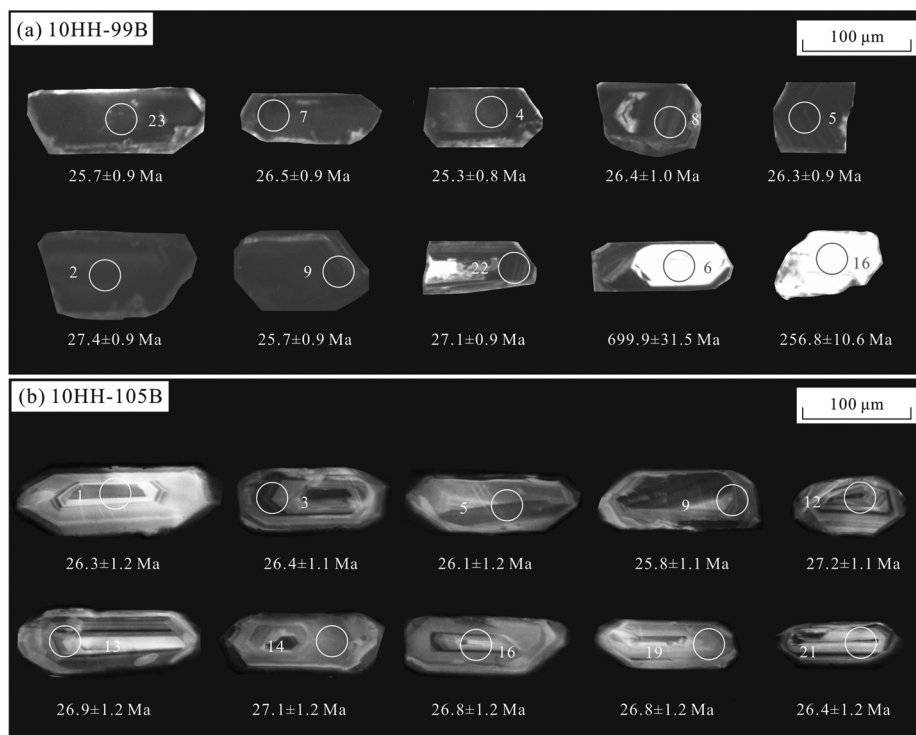


图 3 哀牢山红河剪切带花岗岩 (a) 10HH-99B 和 (b) 10HH-105B 代表性锆石 CL 图像
Fig. 3 The cathodoluminescence (CL) images of representative zircons from the granitic rocks of (a) 10HH-99B and (b) 10HH-105B from Ailaoshan-Red River shear zone

表 1 哀牢山构造带甲寅地区花岗质岩石 LA-ICP-MS 锆石 U-Pb 年龄数据

Table 1 LA-ICP-MS zircon U-Pb dating results for granitic rocks from Jiayin area of Ailaoshan-Red River tectonic zone

样品	分析点	Th/U	同位素质量分数比				加权平均年龄/Ma			
			$^{207}\text{Pb}/^{235}\text{U}$	$\pm 1\sigma$	$^{206}\text{Pb}/^{238}\text{U}$	$\pm 1\sigma$	$^{207}\text{Pb}/^{235}\text{U}$	$\pm 1\sigma$	$^{206}\text{Pb}/^{238}\text{U}$	$\pm 1\sigma$
H H 99 B	02	0.14	0.026 5	0.001 2	0.004 3	0.000 1	26.6	1.2	27.4	0.9
	04	0.18	0.027 5	0.001 3	0.003 9	0.000 1	27.6	1.3	25.3	0.8
	05	0.15	0.024 9	0.001 2	0.004 1	0.000 1	25.0	1.2	26.3	0.9
	06	0.20	1.063 3	0.060 2	0.114 7	0.005 5	735.5	29.6	699.9	31.5
	07	0.12	0.028 2	0.001 4	0.004 1	0.000 1	28.2	1.4	26.5	0.9
	08	0.11	0.028 0	0.001 8	0.004 1	0.000 2	28.1	1.8	26.4	1.0
	09	0.20	0.024 6	0.001 2	0.004 0	0.000 1	24.7	1.2	25.7	0.9
	11	0.18	0.025 0	0.001 3	0.003 9	0.000 1	25.1	1.3	24.9	0.8
	12	0.18	0.028 6	0.001 7	0.004 2	0.000 1	28.6	1.7	27.1	1.0
	13	1.54	0.206 0	0.011 7	0.029 9	0.001 0	190.2	9.9	190.0	6.5
	14	0.58	0.239 3	0.019 0	0.037 0	0.001 5	217.9	15.5	234.4	9.4
	15	0.33	0.311 6	0.022 2	0.047 4	0.001 9	275.4	17.2	298.7	11.6
	16	0.47	0.264 7	0.023 1	0.040 6	0.001 7	238.4	18.6	256.8	10.6
	18	0.60	0.041 1	0.006 5	0.006 2	0.000 4	40.9	6.3	40.1	2.8
	21	0.19	0.045 6	0.003 3	0.006 2	0.000 3	45.3	3.2	40.0	2.1
	22	0.14	0.029 7	0.001 6	0.004 2	0.000 1	29.7	1.6	27.1	0.9
	23	0.16	0.030 4	0.001 7	0.004 0	0.000 1	30.4	1.7	25.7	0.9
	24	0.14	0.026 2	0.001 5	0.004 3	0.000 2	26.3	1.5	27.5	1.0
	25	0.15	0.031 0	0.002 3	0.004 0	0.000 1	31.0	2.3	25.4	0.9
	H H 105 B	01	0.11	0.030 8	0.003 2	0.004 1	0.000 2	30.8	3.2	26.3
02		0.14	0.041 5	0.007 2	0.004 6	0.000 4	41.3	7.0	29.6	2.8
03		0.14	0.031 1	0.003 3	0.004 1	0.000 2	31.1	3.2	26.4	1.1
05		0.14	0.030 6	0.003 7	0.004 0	0.000 2	30.6	3.7	26.1	1.2
07		0.19	0.037 1	0.005 1	0.004 4	0.000 2	37.0	5.0	28.1	1.4
08		0.11	0.025 1	0.003 3	0.003 8	0.000 2	25.2	3.3	24.3	1.2
09		0.15	0.029 4	0.002 8	0.004 0	0.000 2	29.5	2.8	25.8	1.1
10		0.15	0.027 3	0.003 0	0.004 3	0.000 2	27.4	3.0	27.5	1.5
11		0.28	0.037 0	0.003 9	0.004 0	0.000 2	36.9	3.8	25.5	1.2
12		0.12	0.027 4	0.003 1	0.004 2	0.000 2	27.4	3.1	27.2	1.1
13		0.10	0.035 3	0.004 0	0.004 2	0.000 2	35.2	4.0	26.9	1.2
14		0.17	0.034 4	0.004 5	0.004 2	0.000 2	34.3	4.4	27.1	1.2
15		0.21	0.036 6	0.004 6	0.004 5	0.000 2	36.5	4.5	29.0	1.2
16		0.40	0.029 7	0.003 4	0.004 2	0.000 2	29.7	3.3	26.8	1.2
17		0.44	0.240 1	0.011 1	0.035 1	0.001 4	218.5	9.1	222.1	8.7
18		0.16	0.037 4	0.004 4	0.004 3	0.000 3	37.3	4.3	27.7	1.8
19		0.11	0.033 5	0.002 7	0.004 2	0.000 2	33.5	2.7	26.8	1.2
20		0.17	0.036 2	0.004 0	0.003 9	0.000 2	36.2	3.9	25.2	1.1
21		0.16	0.028 5	0.002 6	0.004 1	0.000 2	28.5	2.6	26.4	1.2
22		0.14	0.036 1	0.004 2	0.004 5	0.000 3	36.0	4.1	29.0	1.7
23		0.19	0.037 4	0.003 8	0.004 4	0.000 2	37.3	3.7	28.2	1.1
24		0.46	0.034 9	0.008 2	0.004 1	0.000 3	34.8	8.1	26.5	2.1
25		0.17	0.033 2	0.003 1	0.004 4	0.000 2	33.2	3.1	28.4	1.3

10HH-405B 样品锆石晶面整洁光滑, 大部分呈自形的长柱状, 少量存在继承性锆石核, 直径在 50 ~ 220 μm 之间, 长短轴之比一般大于 2。在 CL 图像上大部分锆石显示出典型的震荡生长环带, 表明其为典型的岩浆锆石 (图 3b)。对浅色脉体的 23 个锆石颗粒进行了分析, 所选测点晶形较好, 同时避开裂纹和包裹体。测点 17 的 Th/U 比值为 0.44, 并给出了 222.1 ± 8.7 Ma 的 $^{206}\text{Pb}/^{238}\text{U}$ 年龄值。该测点位于锆石核部, 可能代表前期热事件中残留的锆石。剩余 22 个测点 Th/U 比值在 0.11 ~ 0.46, 投点均落在谐和线上或其附近, 它们的 $^{206}\text{Pb}/^{238}\text{U}$ 加权平均年龄值为 26.8 ± 0.5 Ma (MSWD = 0.94; 图 4b)。这一年龄代表混合岩化浅色花岗岩脉的岩浆结晶年龄。

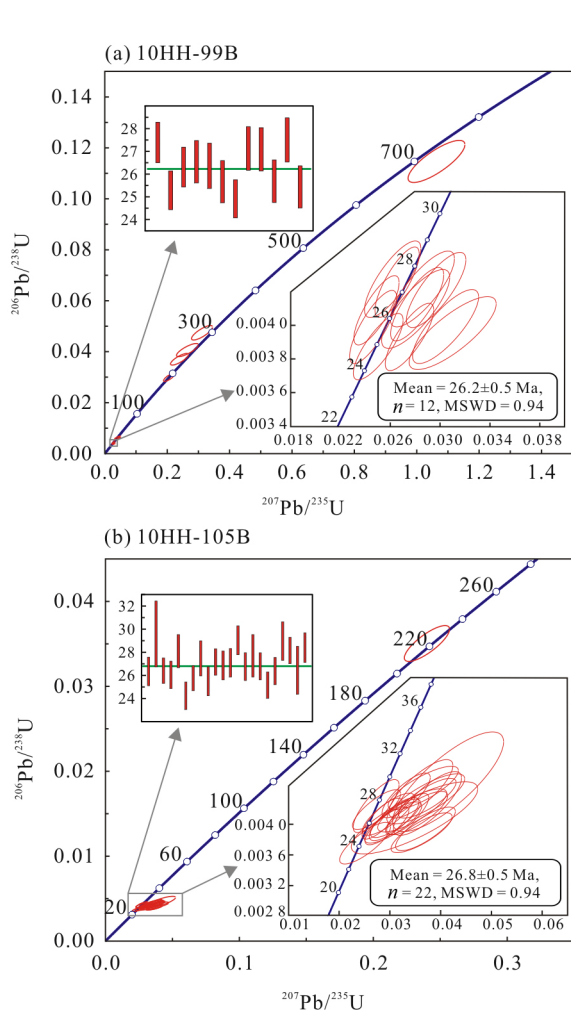


图 4 哀牢山红河剪切带花岗质岩石 (a) 10HH-99B 和 (b) 10HH-105B LA-ICP-MS 锆石 U-Pb 定年结果
Fig. 4 Zircon LA-ICP-MS U-Pb isotopic data for granitic rocks of (a) 10HH-99B and (b) 10HH-105B from Ailaoshan-Red River shear zone

3.2 锆石 Lu-Hf 同位素分析

两个样品的 LA-ICP-MS 锆石 Lu-Hf 同位素组成见表 2。

变形花岗岩 10HH-99B: 进行了 17 颗锆石的原位 Lu-Hf 同位素分析, 按 $t = 26.2$ Ma 的形成年龄, 对其中 12 颗锆石计算出的 $\varepsilon_{\text{Hf}}(t)$ 为 $+0.3 \sim +6.9$, 平均 $+3.4$, 其二阶模式年龄 T_{DM2} 介于 526 ~ 853 Ma 之间。其中 10HH-99B-06 继承锆石给出最老 $^{206}\text{Pb}/^{238}\text{U}$ 表面年龄 699.9 ± 31.5 Ma, 它的 $\varepsilon_{\text{Hf}}(t)$ 和 T_{DM2} 值分别为 -2.99 和 1 575 Ma。剩余 4 颗继承锆石 $^{206}\text{Pb}/^{238}\text{U}$ 表面年龄在 190 ~ 298 Ma 变化, $\varepsilon_{\text{Hf}}(t)$ 介于 $-9.25 \sim -2.81$, T_{DM2} 介于 1.23 ~ 1.58 Ga, 如图 5a 和图 6 所示。

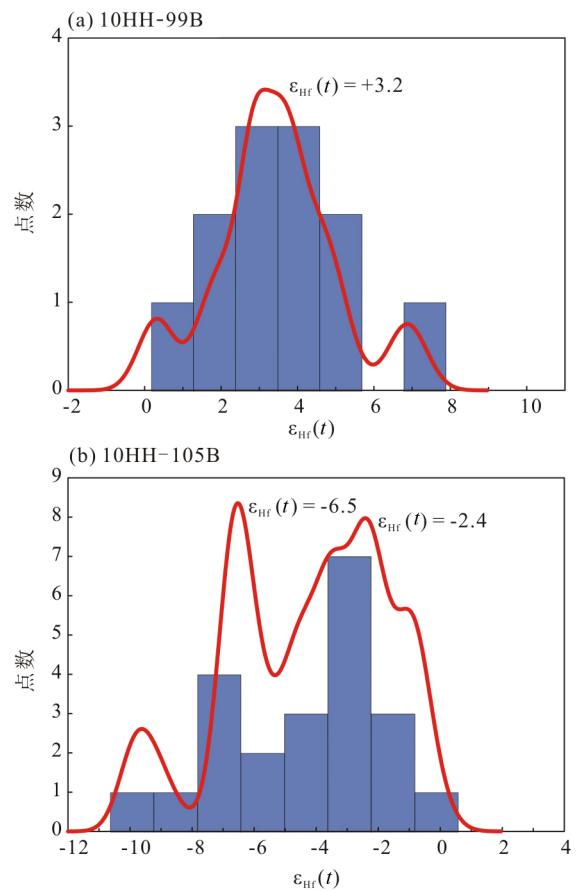


图 5 哀牢山红河剪切带渐新世花岗质岩石 (a) 10HH-99B 和 (b) 10HH-105B 锆石 Hf 同位素组成

Fig. 5 Zircon Hf isotopic compositions for granitic rocks of (a) 10HH-99B and (b) 10HH-105B from Ailaoshan-Red River shear zone

表 2 哀牢山构造带甲寅地区花岗质岩石 LA-ICP-MS 锆石 Lu-Hf 同位素数据

Table 2 LA-ICP-MS zircon Lu-Hf isotopic compositions for granitic rocks from Jiayin area of Ailaoshan-Red River tectonic zone

样品	分析点年龄/Ma	$^{176}\text{Yb}/^{177}\text{Hf}$	$^{176}\text{Lu}/^{177}\text{Hf}$	$^{176}\text{Hf}/^{177}\text{Hf}$	2σ	$^{176}\text{Hf}/^{177}\text{Hf}_i$	$\varepsilon_{\text{Hf}}(0)$	$\varepsilon_{\text{Hf}}(t)$	2σ	T_{DM1}	T_{DM2}	$f_{\text{Lu/Hf}}$		
H H 99 B	02	26.2	0.187 216	0.006 449	0.282 839	0.000 021	0.282 836	2.4	2.8	0.7	686	728	-0.81	
	04	26.2	0.145 783	0.004 988	0.282 864	0.000 025	0.282 861	3.2	3.7	0.9	616	683	-0.85	
	05	26.2	0.133 918	0.004 687	0.282 855	0.000 026	0.282 853	2.9	3.4	0.9	625	698	-0.86	
	06	699.9	0.052 656	0.001 789	0.282 275	0.000 032	0.282 251	-17.6	-3.0	1.1	1 410	1 575	-0.95	
	07	26.2	0.141 594	0.004 933	0.282 858	0.000 031	0.282 856	3.1	3.5	1.1	624	692	-0.85	
	08	26.2	0.114 497	0.004 090	0.282 808	0.000 028	0.282 806	1.3	1.8	1.0	686	780	-0.88	
	09	26.2	0.153 338	0.005 192	0.282 767	0.000 027	0.282 764	-0.2	0.3	0.9	774	853	-0.84	
	11	26.2	0.223 868	0.007 677	0.282 874	0.000 030	0.282 870	3.6	4.0	1.1	653	668	-0.77	
	12	26.2	0.121 412	0.004 263	0.282 840	0.000 026	0.282 837	2.4	2.9	0.9	641	725	-0.87	
	13	190.0	0.092 342	0.002 955	0.282 440	0.000 029	0.282 429	-11.7	-8.0	1.0	1 212	1 397	-0.91	
	14	234.4	0.066 624	0.002 357	0.282 507	0.000 034	0.282 496	-9.4	-4.6	1.2	1 095	1 269	-0.93	
	15	298.7	0.051 167	0.001 747	0.282 517	0.000 030	0.282 507	-9.0	-2.8	1.1	1 062	1 233	-0.95	
	16	256.8	0.013 615	0.000 498	0.282 354	0.000 028	0.282 351	-14.8	-9.3	1.0	1 253	1 516	-0.98	
	22	26.2	0.151 109	0.005 289	0.282 9 53	0.000 029	0.282 950	6.4	6.9	1.0	479	526	-0.84	
	23	26.2	0.171 827	0.005 892	0.282 896	0.000 031	0.282 893	4.4	4.9	1.1	580	627	-0.82	
	24	26.2	0.212 283	0.007 280	0.282 893	0.000 031	0.282 889	4.3	4.7	1.1	612	633	-0.78	
	25	26.2	0.167 676	0.005 872	0.282 824	0.000 032	0.282 821	1.8	2.3	1.1	698	754	-0.82	
	H H 105 B	01	26.8	0.016 300	0.000 627	0.282 498	0.000 037	0.282 498	-9.7	-9.1	1.3	1 057	1 319	-0.98
		02	26.8	0.010 756	0.000 394	0.282 634	0.000 036	0.282 633	-4.9	-4.3	1.3	863	1 082	-0.99
		03	26.8	0.018 728	0.000 683	0.282 585	0.000 038	0.282 585	-6.6	-6.0	1.3	936	1 167	-0.98
		05	26.8	0.026 990	0.000 977	0.282 593	0.000 038	0.282 592	-6.3	-5.8	1.3	934	1 154	-0.97
		07	26.8	0.020 439	0.000 738	0.282 733	0.000 038	0.282 733	-1.4	-0.8	1.3	731	908	-0.98
		08	26.8	0.016 934	0.000 647	0.282 567	0.000 031	0.282 566	-7.3	-6.7	1.1	962	1 199	-0.98
		09	26.8	0.024 138	0.000 870	0.282 663	0.000 037	0.282 662	-3.9	-3.3	1.3	833	1 032	-0.97
		10	26.8	0.028 880	0.000 997	0.282 567	0.000 035	0.282 566	-7.3	-6.7	1.2	970	1 199	-0.97
11		26.8	0.021 509	0.000 778	0.282 736	0.000 038	0.282 736	-1.3	-0.7	1.3	727	903	-0.98	
12		26.8	0.021 066	0.000 775	0.282 631	0.000 033	0.282 630	-5.0	-4.4	1.2	875	1 088	-0.98	
13		26.8	0.016 649	0.000 632	0.282 477	0.000 030	0.282 477	-10.4	-9.8	1.1	1 086	1 355	-0.98	
14		26.8	0.019 974	0.000 724	0.282 688	0.000 036	0.282 687	-3.0	-2.4	1.2	794	988	-0.98	
15		26.8	0.024 316	0.000 873	0.282 691	0.000 031	0.282 690	-2.9	-2.3	1.1	793	983	-0.97	
16		26.8	0.030 211	0.001 061	0.282 712	0.000 036	0.282 711	-2.1	-1.6	1.2	768	946	-0.97	
17		222.1	0.101 786	0.003 277	0.282 526	0.000 028	0.282 512	-8.7	-4.3	1.0	1 094	1 244	-0.90	
18		26.8	0.020 298	0.000 727	0.282 689	0.000 032	0.282 688	-2.9	-2.4	1.1	793	986	-0.98	
19		26.8	0.018 957	0.000 711	0.282 565	0.000 026	0.282 564	-7.3	-6.8	0.9	966	1 203	-0.98	
20		26.8	0.019 734	0.000 705	0.282 688	0.000 032	0.282 688	-3.0	-2.4	1.1	794	988	-0.98	
21		26.8	0.027 464	0.000 980	0.282 654	0.000 027	0.282 654	-4.2	-3.6	1.0	847	1 046	-0.97	
22		26.8	0.016 974	0.000 624	0.282 575	0.000 027	0.282 574	-7.0	-6.4	1.0	950	1 186	-0.98	
23		26.8	0.022 228	0.000 798	0.282 660	0.000 029	0.282 660	-3.9	-3.4	1.0	834	1 036	-0.98	
24		26.8	0.020 246	0.000 728	0.282 731	0.000 028	0.282 730	-1.5	-0.9	1.0	734	912	-0.98	
25		26.8	0.025 970	0.000 944	0.282 623	0.000 033	0.282 623	-5.3	-4.7	1.2	890	1 101	-0.97	

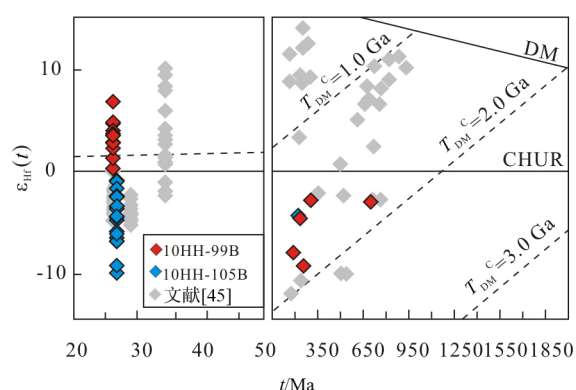


图 6 哀牢山红河剪切带渐新世花岗质岩石锆石 $\varepsilon_{\text{Hf}}(t) - t$ 图解

Fig. 6 $\varepsilon_{\text{Hf}}(t)$ vs. t diagrams for granitic rocks of 10HH-99B and 10HH-105B from Ailaoshan-Red River shear zone

混合岩脉体 10HH-105B: 进行了 23 颗锆石的原位 Lu-Hf 同位素分析, 其中 17 为继承锆石, $\varepsilon_{\text{Hf}}(t)$ 为 -4.3、 T_{DM2} 为 1 244 Ma。其余 22 个分析点 $^{176}\text{Hf}/^{177}\text{Hf} = 0.282 477 \sim 0.282 736$ 。按 $t = 26.8$ Ma 的形成年龄, $\varepsilon_{\text{Hf}}(t) = -9.8 \sim -0.7$, 平均 -4.3, 二阶模式年龄 T_{DM2} 介于 903 ~ 1 355 Ma, 如图 5b 和图 6。

4 讨 论

4.1 成岩过程

近年来, 在金沙江-哀牢山构造带识别出许多新生代岩浆岩, 为研究壳幔相互作用提供了丰富的地球化学信息^[15, 22, 31]。这些新生代岩浆岩以花岗质岩石为主, 普遍具有富钾的特征, 其锆石 Hf 二

阶段模式年龄集中在 1078 ~ 1448 Ma, 与哀牢山构造带内的前寒武纪变质岩系的 Nd 同位素模式年龄接近^[7, 30, 43-44], 被认为是中元古代地壳物质重熔再造形成的, 幔源物质贡献较少^[15, 31, 45]。我们对哀牢山构造带红河甲寅地区花岗质岩石 Lu-Hf 同位素组成的测试结果表明, 样品 10HH-99B 初始 ε_{Hf} 值变化在 +0.3 ~ +6.9 之间, 对应的二阶段 Hf 模式年龄落在 526 ~ 853 Ma 之间, 明显大于锆石的²⁰⁶Pb/²³⁸U 表面年龄, 与 Liu et al.^[19] 提出的哀牢山新生基性下地壳模式年龄一致, 表明该花岗岩与滑石板高 $\varepsilon_{\text{Nd}} - \varepsilon_{\text{Hf}}$ 花岗岩具有相似的源区, 主要源于 526 ~ 853 Ma 新生地壳的重熔。另一件样品 (10HH-105B) 初始 ε_{Hf} 值变化在 -9.8 ~ -0.7 之间, 对应的 Hf 模式年龄落在 903 ~ 1355 Ma 之间, 远大于其结晶年龄。锆石具负 $\varepsilon_{\text{Hf}}(t)$ 值和古老的 Hf 两阶段模式年龄, 揭示其源区主要为古老陆壳物质, 可能来源于哀牢山高级变质带中新元古代地壳物质的部分熔融^[21, 46]。因此, 哀牢山构造带存在前寒武纪结晶基底, 说明代表该区基底的哀牢山群形成时代包括中新元古代, 综合显生宙时期各类岩石, 可知哀牢山高级变质带是一个杂岩。结合区域构造演化, 我们认为该花岗岩形成可能与印欧板块后碰撞背景下古老地壳熔融相关, 是造山带在渐新世时期剪切过程因伸展松弛而发生减压熔融的产物。Lin et al.^[45] 在点苍山和哀牢山也识别出了晚渐新世低 $\varepsilon_{\text{Hf}}(t)$ 片麻岩 (图 8), 其成因应与本文低 $\varepsilon_{\text{Hf}}(t)$ 花岗岩相似。综合可知, 低 $\varepsilon_{\text{Hf}}(t)$ 的花岗岩源区可能是元古宙哀牢山群变质杂砂岩, 高 $\varepsilon_{\text{Hf}}(t)$ 的花岗岩源自软流圈地幔热源加热新生下地壳的部分熔融^[19, 47]。

Rapp & Watson^[48] 的实验表明变质玄武岩熔融的最低温度为 1000 °C, 地壳加厚和中下地壳的放射性元素生热显然无法产生这么高的温度, 那么基性下地壳熔融的热源来自哪里? 哀牢山构造带是特提斯-喜马拉雅构造域的重要地区, 在青藏高原东南缘新生代以来的构造演化讨论中, 围绕哀牢山构造带对印欧碰撞的响应机制一直存在诸多争议。目前, 主要争论的焦点在于三江地区广泛分布的大型走滑断层在大陆挤压过程中扮演着怎样的角色^[49]。一种观点认为, 印度板块本质上是刚性的岩石圈块体, 其变形主要集中在板块的边缘, 红河断裂带是大陆块体侧向逃逸的东部边界。因此, 走滑断层切割深达岩石圈地幔^[12, 14, 50-52]。另一种观点认为挤压加厚的陆壳是一种薄的粘性席体, 其内部变形是

均匀的, 主体上是非旋转岩石圈缩短, 故而走滑断层纯粹是在地壳尺度^[53-57]。此外需要注意的是, 华南的大部分研究地区普遍受陆内深断裂的控制, 许多深断裂继承了古俯冲带、古拼接带等板块边界构造, 在后来发生的部分熔融事件中, 新生岩浆继承了早先形成的与俯冲和碰撞有关的含有较多幔源物质的特征, 在地球化学方面显示幔源组分参与特征^[58]。Zhang 和 Schärer^[15] 认为在哀牢山-红河左旋走滑剪切过程中存在热异常。因此, 处于后碰撞环境的研究区, 最有可能的深部热源就是上地幔尺度上的深大断裂。此外, 哀牢山富碱侵入岩不管是由古洋壳板块加岩石圈地幔部分熔融形成^[59-61], 还是印欧板块俯冲过程中板片断离导致软流圈物质上涌诱发加厚大陆下地壳部分熔融形成^[62-63], 均是处在强烈的区域性构造应力转换阶段^[64], 可能深切至上地幔的大型走滑断裂系统是富碱斑岩岩浆的重要运移通道, 也是地壳部分熔融的重要热源之一。我们认为, 两类花岗岩的形成过程如下: 在渐新世后碰撞构造环境中, 地壳拉张和深大断裂活动导致地幔上涌, 高 $\varepsilon_{\text{Hf}}(t)$ 花岗岩由被底侵的玄武质下地壳物质部分熔融形成, 其热源可能是底侵的幔源镁铁质岩浆。受碰撞作用的影响, 因地壳加厚及阶段性剪切作用, 导致地壳重熔产生低 $\varepsilon_{\text{Hf}}(t)$ 花岗岩, 岩石部分熔融的热源来自于块体的摩擦运动。

4.2 两类晚渐新世花岗岩的构造指示

近年来, 哀牢山红河剪切带众多高封闭温度同位素体系的年代学, 如独居石、锆石 U-Th-Pb 定年的研究, 显示其经历了一个复杂的热历史 (图 7)。该区域发表的大部分花岗质岩石 U-Pb 年龄集中在 35 ~ 21 Ma, 最老年龄在 35 ~ 38 Ma^[15, 22-23, 65-67]。同时, 研究区同剪切矿物的⁴⁰Ar/³⁹Ar 定年结果给出了 32 ~ 22 Ma 的年龄范围^[15, 68-69]。结合青藏高原东南、滇西地区以及越南地区广泛存在的高钾质岩浆岩, Liang et al.^[70] 认为初始左旋走滑运动发生在 35 ~ 36 Ma。基于变质岩、热年代学数据不少学者提出初始左旋剪切至少在 35 Ma^[15, 71-72]。我们对云南红河甲寅地区两类花岗质岩石研究结果显示, 在晚渐新世存在一期岩浆岩的作用, 并且同时软流圈地幔的上侵说明此时哀牢山局部地区可能转化为伸展背景, 也就是说红河剪切带剪切作用在晚渐新世由压剪转为扭剪作用。这一结论也为我们在深变质带内识别的 26 Ma 变基性岩所证明 (课题组待刊数据)。

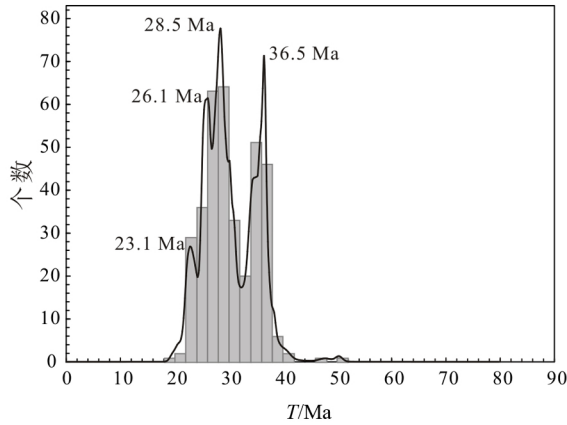


图 7 哀牢山红河剪切带新生代岩石锆石 U-Pb 年龄谱系图
数据来源于文献 [22-23, 31, 45, 73-77] 以及本研究
Fig. 7 Zircon U-Pb age histograms for the Cenozoic rocks
from the Ailaoshan-Red River shear zone
Age data refer to the following sources:
[22-23, 31, 45, 73-77] and this study

结合邻近的大地构造格局来看 (图 8), 哀牢山红河剪切带位于印支和扬子板块交界处, 高黎贡山右旋走滑断裂带位于腾冲地块和保山地块间, 是思茅-印支地块的西边界断层。这些韧性剪切带可能与红河剪切带一致, 都是切穿至岩石圈地幔深度的断裂带。Wang et al. [78] 认为右旋的高黎贡山剪切带和左旋的崇山剪切带始于 ~ 32 Ma, 终止于约 15 ~ 17 Ma。同样不同学者对糜棱岩、片麻岩、花岗质脉中不同矿物进行同位素定年的结果表明, 高黎贡山峰期变质时间介于 38 ~ 22 Ma 之间 [79-81]。哀牢山红河剪切带剪切作用可能与高黎贡山右旋走滑剪切带和崇山左旋走滑剪切带具一致延续时限, 它们都是新生代以来印欧板块碰撞造山事件在青藏高原东南缘的响应。高黎贡山剪切带和哀牢山红河剪切带肢解了至少两大块体 (兰坪思茅地体和掸泰地块) (图 8), 而不是由 Tapponnier et al. [12] 提出的东南缘各陆块为一个单一的刚性块体 [82-83]。

5 结 论

1) 云南红河甲寅地区识别出两类晚渐新世 (~26 Ma) 花岗质岩石, 其锆石 $\varepsilon_{\text{Hf}}(t)$ 平均值分别为 +3.4 和 -4.3, 二阶段模式年龄分别为 526 ~ 853 Ma 和 903 ~ 1 355 Ma。前者源自新生基性下地壳的部分熔融, 后者源岩为元古宙哀牢山群变质杂砂岩。

2) 甲寅两类晚渐新世花岗岩的发现说明哀牢山群并不全是扬子板块的元古代结晶基底, 也包含

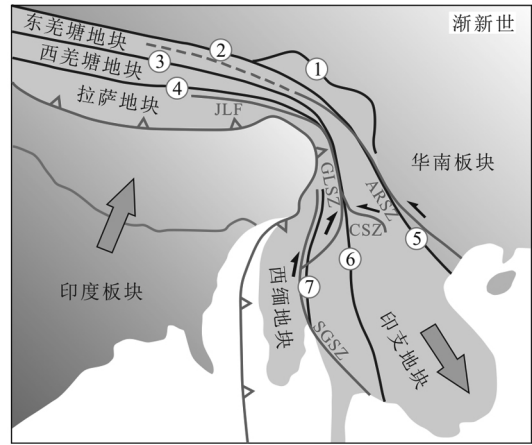


图 8 三江地区渐新世时期印支地块沿剪切带东南向挤出被肢解成不同的块体 (改自 [84])

① 甘孜理塘缝合带; ② 金山江缝合带; ③ 龙木错-双湖缝合带; ④ 班公湖怒江缝合带; ⑤ 哀牢山缝合带; ⑥ 昌宁-孟连缝合带; ⑦ 密支那缝合带. GLSZ = 高黎贡山剪切带; CSZ = 崇山剪切带; ARSZ = 哀牢山-红河剪切带; SGSZ = 实皆剪切带; JLF = 嘉黎断裂

Fig. 8 Distribution of the late Oligocene shear zones in Southeast Asia (revised from [84])

① Garzê-Litang suture; ② Jinshajiang suture; ③ Longmu Tso-Shuanghu suture; ④ Banggong-Nujiang suture; ⑤ Ailaoshan suture; ⑥ Changning-Menglian suture; ⑦ Myitkiyina suture

GLSZ = Gaoligongshan shear zone; CSZ = Chongshan shear zone; ARSZ = Ailaoshan-Red River shear zone; JLF = Jiali fault; SGSZ = Saging shear zone

有新生代岩浆岩。

3) 甲寅两类花岗岩的发现还说明红河剪切带在晚渐新世切穿了岩石圈地幔, 为我们认识东南亚陆块属性及南海打开提供了资料。

致谢: 野外样品采集以及室内岩石分析工作得到蔡永丰、张爱梅等的帮助, 编辑部老师和评审专家的意见, 对提高论文质量起了重要作用, 在此一并致以诚挚谢意。

参考文献:

[1] ŞENGÖR A M C, ALTINER D, CIN A, et al. Origin and assembly of the Tethyside orogenic collage at the expense of Gondwana Land [J]. Special Publications of Geological Society of London, 1988, 37: 119-181.
[2] 莫宣学, 路凤香, 沈上越, 等. 三江特提斯火山作用与成矿 [M]. 北京: 地质出版社, 1993.
[3] JIAN P, LIU D Y, KRÖNER A, et al. Devonian to Permian plate tectonic cycle of the Paleo-Tethys Orogen in southwest China (I): Geochemistry of ophiolites, arc/back-arc assemblages and within-plate igneous rocks [J].

- Lithos, 2009, 113(3/4): 748–766.
- [4] JIAN P, LIU D Y, KRÖNER A, et al. Devonian to Permian plate tectonic cycle of the Paleo-Tethys Orogen in southwest China (II): Insights from zircon ages of ophiolites, arc/back-arc assemblages and within-plate igneous rocks and generation of the Emeishan CFB province [J]. Lithos, 2009, 113(3/4): 767–784.
- [5] WANG Y J, ZHANG A M, FAN W M, et al. Petrogenesis of late Triassic post-collisional basaltic rocks of the Lancangjiang tectonic zone, southwest China, and tectonic implications for the evolution of the eastern Paleotethys: geochronological and geochemical constraints [J]. Lithos, 2010, 120(3): 529–546.
- [6] LIU H C, WANG Y J, CAWOOD P A, et al. Record of Tethyan ocean closure and Indosinian collision along the Ailaoshan suture zone (SW China) [J]. Gondwana Research, 2014, 27(3): 1292–1306.
- [7] 钟大赉. 滇川西部古特提斯造山带 [M]. 北京: 科学出版社, 1998.
- ZHONG D L. Paleo-Tethyan orogenic belt in the western parts of the Sichuan and Yunnan provinces [M]. Beijing: Science Press, 1998.
- [8] METCALFE I. Gondwanaland dispersion, Asian accretion and evolution of eastern Tethys [J]. Australian Journal of Earth Sciences, 1996, 43(6): 605–623.
- [9] METCALFE I. Tectonic framework and Phanerozoic evolution of Sundaland [J]. Gondwana Research, 2011, 19(1): 3–21.
- [10] METCALFE I. Gondwana dispersion and Asian accretion: tectonic and palaeogeographic evolution of eastern Tethys [J]. Journal of Asian Earth Sciences, 2013, 66: 1–33.
- [11] 刘本培, 冯庆来, CHONGLAKMANI C 等. 滇西古特提斯多岛洋的结构及其南北延伸 [J]. 地学前缘, 2002, 9(3): 161–172.
- LIU B P, FENG Q L, CHONGLAKMANI C. Framework of paleotethyan archipelago ocean of western Yunnan and its elongation towards north and south [J]. Earth Science Frontiers, 2002, 9(3): 161–172.
- [12] TAPPONNIER P, PELTZER G, ARMIJO R. On the mechanics of the collision between India and Asia [J]. Geological Society, London, Special Publications, 1986, 19(1): 113–157.
- [13] TAPPONNIER P, LACASSIN R, LELOUP P H, et al. The Ailao Shan/Red River metamorphic belt: Tertiary left-lateral shear between Indochina and South China [J]. Nature, 1990, 343(6257): 431–437.
- [14] LELOUP P H, LACASSIN R, TAPPONNIER P, et al. The Ailao Shan-Red River shear zone (Yunnan, China), Tertiary transform boundary of Indochina [J]. Tectonophysics, 1995, 251(s1–4): 3–10.
- [15] ZHANG L S, SCHÄRER U. Age and origin of magmatism along the Cenozoic Red River shear belt, China [J]. Contributions to Mineralogy and Petrology, 1999, 134(1): 67–85.
- [16] 张玉泉, 夏斌, 梁华英, 等. 云南大平糜棱岩化碱性花岗岩的锆石特征及其地质意义 [J]. 高校地质学报, 2004, 10(3): 378–384.
- ZHANG Y Q, XIA B, LIANG H Y, et al. Characteristics of zircons for dating from Daping mylonitized alkaline granite in Yunnan and their geologic implications [J]. Geological Journal of China Universities, 2004, 10(3): 378–384.
- [17] 刘俊来, 王安建, 曹淑云, 等. 滇西点苍山杂岩中混合岩的地质年代学分析及其区域构造内涵 [J]. 岩石学报, 2008, 24(3): 413–420.
- LIU J L, WANG A J, CAO S Y, et al. Geochronology and tectonic implication of migmatites from Diancangshan, Western Yunnan [J]. Acta Petrologica Sinica, 2008, 24(3): 413–420.
- [18] QI X X, ZENG L S, ZHU L H, et al. Zircon U-Pb and Lu-Hf isotopic systematics of the Daping plutonic rocks: Implications for the Neoproterozoic tectonic evolution of the northeastern margin of the Indochina block, Southwest China [J]. Gondwana Research, 2012, 21(1): 180–193.
- [19] LIU H C, WANG Y J, FAN W M, et al. Petrogenesis and tectonic implications of Late-Triassic high $\varepsilon_{Nd}(t) - \varepsilon_{Hf}(t)$ granites in the Ailaoshan tectonic zone (SW China) [J]. Science China Earth Sciences, 2014, 57(9): 2181–2194.
- [20] CAI Y F, WANG Y J, CAWOOD P A, et al. Neoproterozoic subduction along the Ailaoshan zone, South China: Geochronological and geochemical evidence from amphibolite [J]. Precambrian Research, 2014, 245(5): 13–28.
- [21] CAI Y F, WANG Y J, CAWOOD P A, et al. Neoproterozoic crustal growth of the Southern Yangtze Block: Geochemical and zircon U-Pb geochronological and Lu-Hf isotopic evidence of Neoproterozoic diorite from the Ailaoshan zone [J]. Precambrian Research, 2015, 266: 137–149.
- [22] CAO S Y, LIU J L, LEISS B, et al. Oligo-Miocene shearing along the Ailao Shan-Red River shear zone: constraints from structural analysis and zircon U/Pb geochronology of magmatic rocks in the Diancang Shan massif, SE Tibet, China [J]. Gondwana Research, 2011, 19(4): 975–993.

- [23] TANG Y, LIU J L, TRAN M D, et al. Timing of left-lateral shearing along the Ailao Shan-Red River shear zone: constraints from zircon U-Pb ages from granitic rocks in the shear zone along the Ailao Shan Range, Western Yunnan, China [J]. *International Journal of Earth Sciences*, 2013, 102(3): 605–626.
- [24] PENG T P, WANG Y J, ZHAO G C, et al. Arc-like volcanic rocks from the southern Lancangjiang zone, SW China: Geochronological and geochemical constraints on their petrogenesis and tectonic implications [J]. *Lithos*, 2008, 102(1/2): 358–373.
- [25] WANG Y J, ZHANG A M, FAN W M, et al. Petrogenesis of late Triassic post-collisional basaltic rocks of the Lancangjiang tectonic zone, southwest China, and tectonic implications for the evolution of the eastern Paleotethys: Geochronological and geochemical constraints [J]. *Lithos*, 2010, 120(3/4): 529–546.
- [26] 云南省地质矿产局. 云南省区域地质志 [M]. 北京: 地质出版社, 1990.
BUREAU OF GEOLOGY AND MINERAL RESOURCES OF YUNNAN PROVINCE. *Regional Geology of Yunnan Province* [M]. Beijing: Geological Publishing House, 1990.
- [27] XIA X P, NIE X S, LAI C K, et al. Where was the Ailaoshan Ocean and when did it open: a perspective based on detrital zircon U-Pb age and Hf isotope evidence [J]. *Gondwana Research*, 2015.
- [28] 翟明国, 从柏林, 乔广生, 等. 中国滇西南造山带变质岩的 Sm-Nd 和 Rb-Sr 同位素年代学 [J]. *岩石学报*, 1990, 6(4): 1–11.
ZHAI M G, CONG B L, QIAO G S, et al. Sm-Nd and Rb-Sr geochronology of metamorphic rocks from SW Yunnan orogenic zones, China [J]. *Acta Petrologica Sinica*, 1990, 6(4): 1–11.
- [29] 翟明国, 从柏林. 对于点苍山-石鼓变质带区域划分的意见 [J]. *岩石学报*, 1993, 9(3): 227–239.
ZHAI M G, CONG B L. The Diancangshan-Shigu metamorphic belt in W. Yunnan, China: their geochemical and geochronological characteristics and division of metamorphic domains [J]. *Acta Petrologica Sinica*, 1993, 9(3): 227–239.
- [30] 沙绍礼, 包俊跃, 金亚昌, 等. 点苍山变质带同位素年代学研究新进展 [J]. *云南地质*, 1999, 18(1): 63–66.
SHA S L, BAO J Y, JIN Y C, et al. The new development of isotopic geochronology of the Diancang mountains metamorphic zone [J]. *Yunnan Geology*, 1999, 18(1): 63–66.
- [31] 戚学祥, 赵宇浩, 朱路华, 等. 滇西点苍山构造带新生代岩浆活动及其构造意义 [J]. *岩石学报*, 2014, 30(8): 2217–2228.
QI X X, ZHAO Y H, ZHU L H, et al. Cenozoic magmatism in Diancangshan Range, southwestern Yunnan, China and its tectonic implications [J]. *Acta Petrologica Sinica*, 2014, 30(8): 2217–2228.
- [32] 戚学祥, 朱路华, 李化启, 等. 青藏高原东缘哀牢山-金沙江构造带糜棱状花岗岩的 LA-ICP-MS U-Pb 定年及其构造意义 [J]. *地质学报*, 2010, 84(3): 357–369.
QI X X, ZHU L H, LI H Q, et al. Zircon LA-ICP-MS U-Pb dating for mylonitized granite from the Ailaoshan-Jinshajiang tectonic zone in the eastern Qinghai-Tibet Plateau and its tectonic significance [J]. *Acta Geologica Sinica*, 2010, 84(3): 357–369.
- [33] 李宝龙, 季建清, 付孝悦, 等. 滇西点苍山-哀牢山变质岩系锆石 SHRIMP 定年及其地质意义 [J]. *岩石学报*, 2008, 24(10): 2322–2330.
LI B L, JI J Q, FU X Y, et al. Zircon SHRIMP dating and its geological implications of metamorphic rocks in Ailao Shan-Diancang Mountain Ranges, west Yunnan [J]. *Acta Petrologica Sinica*, 2008, 24(10): 2322–2330.
- [34] 王义昭, 丁俊. 云南哀牢山中深变质岩系构造变形特征及演变 [J]. *沉积与特提斯地质*, 1996, 20: 52–70.
WANG Y Z, DING J. Structural deformation and evolution of the medium-to high-grade metamorphic rock series in the Ailao Mountains, Yunnan [J]. *Sedimentary Geology and Tethyan Geology*, 1996, 20: 52–70.
- [35] 胥颐, 刘建华, 刘福田, 等. 哀牢山-红河断裂带及其邻区的地壳上地幔结构 [J]. *中国科学(D 辑)*, 2003, 33(12): 1201–1208.
XU Y, LIU J H, LIU F T, et al. Crust and upper mantle structure of the Ailao Shan-Red River fault zone and adjacent regions [J]. *Science in China (Series D): Earth Sciences*, 2005, 48(2): 156–164.
- [36] 张进江, 钟大赉, 桑海清, 等. 哀牢山-红河构造带古新世以来多期活动的构造和年代学证据 [J]. *地质科学*, 2006, 41(2): 291–310.
ZHANG J J, ZHONG D L, SANG H Q, et al. Structural and geochronological evidence for multiple episodes of Tertiary deformation along the Ailaoshan-Red River shear zone, Southeastern Asia, since the Paleocene [J]. *Acta Geologica Sinica*, 2006, 80(1): 79–96.
- [37] YUAN H L, GAO S, LIU X M, et al. Accurate U-Pb age and trace element determinations of zircon by Laser Ablation-Inductively Coupled Plasma-Mass Spectrometry [J]. *Geostandards and Geoanalytical Research*, 2004,

- 28(3): 353–370.
- [38] WU F Y, YANG Y H, XIE L W, et al. Hf isotopic compositions of the standard zircons and baddeleyites used in U-Pb geochronology [J]. *Chemical Geology*, 2006, 234(1/2): 105–126.
- [39] 谢烈文, 张艳斌, 张辉煌, 等. 锆石/斜锆石 U-Pb 和 Lu-Hf 同位素以及微量元素成分的同时原位测定 [J]. *科学通报*, 2008, 53(2): 220–228.
XIE L W, ZHANG Y B, ZHANG H H, et al. In situ simultaneous determination of trace elements, U-Pb and Lu-Hf isotopes in zircon and baddeleyite [J]. *Chinese Science Bulletin*, 2008, 53(10): 1565–1573.
- [40] LUDWIG K R. User's manual for Isoplot/Ex, version 3.0, a geochronological toolkit for Microsoft Excel [CP]. Berkeley Geochronology Center, CA, special publication, no. 4 2003.
- [41] LIU Y S, GAO S, HU Z C, et al. Continental and oceanic crust recycling-induced melt-peridotite interactions in the Trans-North China Orogen: U-Pb dating, Hf isotopes and trace elements in zircons from mantle xenoliths [J]. *Journal of Petrology*, 2010, 51(1–2): 537–571.
- [42] 林清茶, 夏斌, 张玉泉, 等. 哀牢山-金沙江碱性岩带南段云南金平八一村钾质碱性花岗岩锆石 SHRIMP U-Pb 年龄 [J]. *地质通报*, 2005, 24(5): 420–423.
LIN Q C, XIA B, ZHANG Y Q, et al. Zircon SHRIMP dating of the Bayicun potassic alkali-granite, Jinping, Yunnan, in the southern segment of the Ailaoshan-Jinshajiang alkaline rock belt [J]. *Regional Geology of China*, 2005, 24(5): 420–423.
- [43] 邹日, 朱炳泉, 孙大中, 等. 红河成矿带壳幔演化与成矿作用的年代学研究 [J]. *地球化学*, 1997, 26(2): 46–56.
ZOU R, ZHU B Q, SUN D Z. Geochronology studies of crust-mantle interaction and mineralization in the Honghe ore deposit zone [J]. *Geochimica*, 1997, 26(2): 46–56.
- [44] 朱炳泉, 常向阳, 邱华宁, 等. 云南前寒武纪基底形成与变质时代及其成矿作用年代学研究 [J]. *前寒武纪研究进展*, 2001, 24(2): 75–68.
ZHU B Q, CHANG X Y, QIU H N, et al. Geochronological study on formation and metamorphism of Precambrian basement and their mineralization in Yunnan, China [J]. *Progress in Precambrian Research*, 2001, 24(2): 75–68.
- [45] LIN T H, CHUNG S L, CHIU H Y, et al. Zircon U-Pb and Hf isotope constraints from the Ailao Shan-Red River shear zone on the tectonic and crustal evolution of southwestern China [J]. *Chemical Geology*, 2012, 291(1): 23–37.
- [46] WANG Y J, ZHOU Y Z, CAI Y F, et al. Geochronological and geochemical constraints on the petrogenesis of the Ailaoshan granitic and migmatite rocks and its implications on Neoproterozoic subduction along the SW Yangtze Block [J]. *Precambrian Research*, 2016, 283: 106–124.
- [47] 刘汇川, 王岳军, 蔡永丰, 等. 哀牢山构造带新安寨晚二叠世末期过铝质花岗岩锆石 U-Pb 年代学及 Hf 同位素组成研究 [J]. *大地构造与成矿学*, 2013, 37(1): 87–98.
LIU H C, WANG Y J, CAI Y F, et al. Zircon U-Pb geochronology and Hf isotopic composition of the Xin'anzhai granite along the Ailaoshan tectonic zone in west Yunnan province [J]. *Geotectonica et Metallogenia*, 2013, 37(1): 87–98.
- [48] RAPP R P, WATSON E B. Dehydration melting of metabasalt at 8–32 kbar: implications for continental growth and crust-mantle recycling [J]. *Journal of Petrology*, 1995, 36(4): 891–931.
- [49] SEARLE M P. Role of the Red River Shear zone, Yunnan and Vietnam, in the continental extrusion of SE Asia [J]. *Journal of the Geological Society*, 2006, 63(6): 1025–1036.
- [50] ARMIJO R, TAPPONNIER P, HAN T L. Late Cenozoic right-lateral strike-slip faulting in southern Tibet [J]. *Journal of Geophysical Research: Solid Earth*, 1989, 94(B3): 2787–2838.
- [51] MOLNAR P, TAPPONNIER P. Cenozoic tectonics of Asia: effects of a continental collision [J]. *Science*, 1975, 189(4201): 419–426.
- [52] PELTZER G, TAPPONNIER P. Formation and evolution of strike-slip faults, rifts, and basins during the India-Asia collision—An experimental approach [J]. *Journal of Geophysical Research: Solid Earth* (1978–2012), 1988, 93(B12): 15085–15117.
- [53] ENGLAND P, MCKENZIE D. A thin viscous sheet model for continental deformation [J]. *Geophysical Journal International*, 1982, 70(2): 295–321.
- [54] ENGLAND P, HOUSEMAN G. Finite strain calculations of continental deformation: 2. Comparison with the India-Asia collision zone [J]. *Journal of Geophysical Research: Solid Earth*, 1986, 91(B3): 3664–3676.
- [55] BURCHFIEL B C, DENG Q D, MOLNAR P, et al. Intracrustal detachment within zones of continental deformation [J]. *Geology*, 1989, 17(8): 748–752.
- [56] HOUSEMAN G, ENGLAND P. Crustal thickening versus lateral expulsion in the Indian-Asian continental col-

- lision [J]. *Journal of Geophysical Research: Solid Earth*, 1993, 98(B7): 12233 – 12249.
- [57] JOLIVET L, BEYSSAC O, GOFFÉ B, et al. Oligo-Miocene midcrustal subhorizontal shear zone in Indochina [J]. *Tectonics*, 2001, 20(1): 46 – 57.
- [58] 华仁民, 陈培荣, 张文兰, 等. 华南中、新生代与花岗岩类有关的成矿系统 [J]. *中国科学 (D 辑)*, 2003, 33(4): 335 – 343.
HUA R M, CHEN P R, ZHANG W L, et al. Metallogenic systems related to Mesozoic and Cenozoic granitoids in South China [J]. *Science in China (Series D): Earth Sciences*, 2003, 46(8): 816 – 829.
- [59] 刘福田, 刘建华, 何建坤, 等. 滇西特提斯造山带下扬子地块的俯冲板片 [J]. *科学通报*, 2000, 45(1): 79 – 65.
LIU F T, LIU J H, HE J K, et al. Subduction slab of lower Yangtze massif in Tethys orogenic belt. West Yunnan [J]. *Chinese Science Bulletin*, 2000, 45(1): 79 – 83.
- [60] 徐兴旺, 蔡新平, 宋保昌, 等. 滇西北衙金矿区碱性斑岩岩石学、年代学和地球化学特征及其成因机制 [J]. *岩石学报*, 2006, 22(3): 631 – 642.
XU X W, CAI X P, SONG B C, et al. Petrologic, chronological and geochemistry characteristics and formation mechanism of alkaline porphyries in the Beiya gold district, western Yunnan [J]. *Acta Petrologica Sinica*, 2006, 22(3): 631 – 642.
- [61] FLOWER M F J, HOANG N, LO C H, et al. Potassic magma genesis and the Ailao Shan-Red River fault [J]. *Journal of Geodynamics*, 2013, 69(Special Issue): 84 – 105.
- [62] 寇彩化, 张招崇, 侯通, 等. 滇西剑川 OIB 型苦橄玢岩: 俯冲板块断离的产物? [J]. *岩石学报*, 2011, 27(9): 2679 – 2693.
KOU C H, ZHANG Z C, HOU T, et al. OIB-type picritic porphyrite from Jianchuan in the western Yunnan Province: Results of break-off of the subducting plate? [J]. *Acta Petrologica Sinica*, 2011, 27(9): 2679 – 2693.
- [63] 和文言, 莫宣学, 喻学惠, 等. 滇西北衙金多金属矿床锆石 U-Pb 和辉钼矿 Re-Os 年龄及其地质意义 [J]. *岩石学报*, 2013, 29(4): 1301 – 1310.
HE W Y, MO X X, YU X H, et al. Zircon U-Pb and molybdenite Re-Os dating for the Beiya gold-polymetallic deposit in the western Yunnan Province and its geological significance [J]. *Acta Petrologica Sinica*, 2013, 29(4): 1301 – 1310.
- [64] WANG J H, YIN A, HARRISON T M, et al. A tectonic model for Cenozoic igneous activities in the eastern Indo-Asian collision zone [J]. *Earth and Planetary Science Letters*, 2001, 188(1): 123 – 133.
- [65] LELOUP P H, ARNAUD N, LACASSIN R, et al. New constraints on the structure, thermochronology, and timing of the Ailao Shan-Red River shear zone, SE Asia [J]. *Journal of Geophysical Research: Solid Earth*, 2001, 106(B4): 6683 – 6732.
- [66] SASSIER C, LELOUP P H, RUBATTO D, et al. Direct measurement of strain rates in ductile shear zones: A new method based on syntectonic dikes [J]. *Journal of Geophysical Research: Solid Earth*, 2009, 114(B1): 549 – 549.
- [67] GUO X F, WANG Y J, LIU H C, et al. Zircon U-Pb geochronology of the Cenozoic granitic mylonite along the Ailaoshan-Red River shear zone: New constraints on the timing of the sinistral shearing. *Journal of Earth Science*, 2016, 27(3): 435 – 443.
- [68] WANG P L, LO C H, CHUNG S L, et al. Onset timing of left-lateral movement along the Ailao Shan-Red River shear zone: $^{40}\text{Ar}/^{39}\text{Ar}$ dating constraint from the Nam Dinh Area, northeastern Vietnam [J]. *Journal of Asian Earth Sciences*, 2000, 18(3): 281 – 292.
- [69] SEARLE M P, YE H M W, LIN T H, et al. Structural constraints on the timing of left-lateral shear along the Red River shear zone in the Ailao Shan and Diancang Shan Ranges, Yunnan, SW China [J]. *Geosphere*, 2010, 6(6): 316 – 338.
- [70] LIANG H Y, CAMPBELL I H, ALLEN C M, et al. The age of the potassic alkaline igneous rocks along the Ailao Shan-Red River shear zone: implications for the onset age of left-lateral shearing [J]. *The Journal of Geology*, 2007, 115(2): 231 – 242.
- [71] SCHÄRER U, ZHANG L S, TAPPONNIER P. Duration of strike-slip movements in large shear zones: the Red River belt, China [J]. *Earth and Planetary Science Letters*, 1994, 126(4): 379 – 397.
- [72] GILLEY L D, HARRISON T M, LELOUP P H, et al. Direct dating of left-lateral deformation along the Red River shear zone, China and Vietnam [J]. *Journal of Geophysical Research: Solid Earth*, 2003, 108(B2): 183 – 185.
- [73] LI B L, JI J Q, WANG D D, et al. Determination of Eocene-Oligocene (30 – 40 Ma) deformational time by zircon U-Pb SHRIMP dating from leucocratic rocks in the Ailao Shan-Red River shear zone, southeast Tibet, China [J]. *International Geology Review*, 2014, 56(1): 74 – 87.
- [74] 赵春强, 赵利, 曹淑云, 等. 点苍山变质杂岩新生代变质-变形演化及其区域构造内涵 [J]. *岩石学报*,

- 2014, 30(3): 851–866.
- ZHAO C Q, ZHAO L, CAO S Y, et al. Cenozoic deformation-metamorphic evolution of the Diancang Shan metamorphic complex and regional tectonic implications [J]. *Acta Petrologica Sinica*, 2014, 30(3): 851–866.
- [75] ZHANG B, ZHANG J J, LIU J, et al. The Xuelongshan high strain zone: Cenozoic structural evolution and implications for fault linkages and deformation along the Ailao Shan-Red River shear zone [J]. *Journal of Structural Geology*, 2014, 69: 209–233.
- [76] LIU F L, WANG F, LIU P H, et al. Multiple partial melting events in the Ailao Shan-Red River and Gaoligong Shan complex belts, SE Tibetan Plateau: zircon U-Pb dating of granitic leucosomes within migmatites [J]. *Journal of Asian Earth Sciences*, 2015, 110: 151–169.
- [77] LIU J L, CHEN X Y, WU W B, et al. New tectono-geochronological constraints on timing of shearing along the Ailao Shan-Red River shear zone: Implications for genesis of Ailao Shan gold mineralization [J]. *Journal of Asian Earth Sciences*, 2015, 103: 70–86.
- [78] WANG Y J, FAN W M, ZHANG Y H, et al. Kinematics and $^{40}\text{Ar}/^{39}\text{Ar}$ geochronology of the Gaoligong and Chongshan shear systems, western Yunnan, China: Implications for early Oligocene tectonic extrusion of SE Asia [J]. *Tectonophysics*, 2006, 418(3): 235–254.
- [79] 季建清, 钟大赉, 张连生. 滇西南新生代走滑断裂运动学、年代学、及对青藏高原东南部块体运动的意义 [J]. *地质科学*, 2000, 35(3): 336–349.
- JI J Q, ZHONG D L, ZHANG L S. Kinematics and dating of Cenozoic strike-slip faults in the Tengchong area, west Yunnan: Implications for the block movement in the southeastern Tibet Plateau [J]. 2000, 35(3): 336–349.
- [80] SONG S G, NIU Y L, WEI C J, et al. Metamorphism, anatexis, zircon ages and tectonic evolution of the Gongshan block in the northern Indochina continent—An eastern extension of the Lhasa Block [J]. *Lithos*, 2010, 120(3): 327–346.
- [81] 季再会, 王立全, 林仕良, 等. 滇西高黎贡剪切带内花岗质糜棱岩 LA-ICP-MS 锆石 U-Pb 年龄及其构造意义 [J]. *地质通报*, 2012, 31(8): 1287–1295.
- LI Z H, WANG L Q, LIN S L, et al. LA-ICP-MS zircon U-Pb age of granitic mylonite in the Gaoligong shear zone of western Yunnan Province and its tectonic significance [J]. *Geological Bulletin of China*, 2012, 31(8): 1287–1295.
- [82] CHEN H H, DOBSON J, HELLER F, et al. Paleomagnetic evidence for clockwise rotation of the Simao region since the Cretaceous: A consequence of India-Asia collision [J]. *Earth & Planetary Science Letters*, 1995, 134(1/2): 203–217.
- [83] ZHANG B, ZHANG J J, ZHONG D L. Structure, kinematics and ages of transpression during strain-partitioning in the Chongshan shear zone, western Yunnan, China [J]. *Journal of Structural Geology*, 2010, 32(4): 445–463.
- [84] DENG J, WANG Q F, LI G J, et al. Cenozoic tectono-magmatic and metallogenic processes in the Sanjiang region, southwestern China [J]. *Earth-Science Reviews*, 2014, 138: 268–29.